

## CORROSION PROTECTION OF TIN USING CARBOXYLATE COATINGS IN A SODIUM CHLORIDE SOLUTION

Ivana Škugor Rončević<sup>1\*</sup>, Nives Vladislavić<sup>1</sup>, Marijo Buzuk<sup>1</sup>, Maša Buljac<sup>2</sup>, Anđela Lukin<sup>3</sup>

<sup>1</sup>*Department of General and Inorganic Chemistry, Faculty of Chemistry and Technology,  
University of Split, Croatia*

<sup>2</sup>*Department of Environmental Chemistry, Faculty of Chemistry and Technology,  
University of Split, Croatia*

<sup>3</sup>*Faculty of Chemistry and Technology, University of Split, Croatia*  
skugor@ktf-split.hr

Tin is a moderately corrosion resistant material that is widely used in tinplate for food and beverage packaging. However, despite its moderately corrosion resistance, the presence of oxidizing agents enhances tin dissolution. The dissolution of metallic tin, especially from the inside of a can body into the food content, has a major influence on the food quality and may cause toxicological effects. To overcome the problem, different chemical compounds are added. The most utilized inhibitors in the food industry are nitrites and nitrates, which are hazardous to human health. The present study aims to investigate the influence of carboxylic acids on the corrosion resistance of tin, since they are present in fruit juices and different foodstuffs. The corrosion protection efficiency of carboxylate coatings is investigated in a sodium chloride solution using electrochemical and spectroscopic techniques. The structural characteristics of the surface coatings are investigated using Fourier transform infrared spectroscopy and optical microscopy.

**Keywords:** tin; corrosion inhibition; carboxylic acids; electrochemical methods

### ЗАШТИТА НА КАЛАЈ ОД КОРОЗИЈА СО ПРИМЕНА НА КАРБОКСИЛАТНИ ОБЛОГИ ВО РАСТВОР ОД НАТРИУМ ХЛОРИД

Калајот е материјал што е умерено отпорен на корозија, а широко се користи за обложување на амбалажа за храна и пијалаци. Меѓутоа, и покрај умерената отпорност на корозија, присуството на оксидациски средства го забрзува растворањето на калајот. Растворањето на металниот калај, особено од внатрешноста на конзервите во храната, има големо влијание врз квалитетот на храната и може да предизвика токсиколошки ефект. За да се надмине овој проблем, се додаваат различни хемиски средства. Најкористените инхибитори во прехранбената индустрија се нитритите и нитратите, кои од своја страна се опасни за човековото здравје. Целта на оваа студија е да се испита влијанието на карбоксилни киселини врз отпорноста на калајот на корозија, бидејќи се присутни во овошните сокови и во разни прехранбени продукти. Ефикасноста на заштитата од корозија на карбоксилните облоги е испитана во раствор од натриум хлорид со примена на електрохемиски и спектроскопски техники. Структурните карактеристики на површинските облоги се испитани со примена на Фуриеовата трансформна инфрацрвена спектроскопија и со оптичка микроскопија.

**Клучни зборови:** калај; инхибиција на корозија; карбоксилни киселини; електрохемиски методи

#### 1. INTRODUCTION

Corrosion control of metals is of technical, economic, environmental and aesthetic importance

[1]. The use of inhibitors is one of the best options for protecting metals and alloys against corrosion [1, 2]. Corrosion inhibitors are substances that effectively reduce the corrosion rate of a metal exposed

to aggressive fluid environments [3]. The applicability of organic compounds as corrosion inhibitors is well recognized. The environmental toxicity of organic corrosion inhibitors has prompted the search for green corrosion inhibitors since they are biodegradable and do not contain heavy metals or other toxic compounds [1]. Metal protection via these organic inhibitors comes from the fact that they adsorb on the metal surface to form a protective layer against corrosive species in the media [4–6]. The efficiency of an inhibitor depends on many factors, such as the nature of the metal surface, the type of corrosive media and the chemical structure of the inhibitor. The chemical structure of the organic inhibitor and its charge density are crucial since they dictate the mode of adsorption on the metal surface and the number of metal-surface-active centers that could be covered [7–9].

Tin is a moderately corrosion resistant material that is extensively used in tinplate [10, 11]. The electrochemical behavior of tin in aqueous solutions is of interest due to its widespread technological application in soft solders, bronze and dental amalgam, in addition to its use as tinplate [11, 12]. Tinplate is light gauge, steel sheet or strip, coated on both sides with commercially pure tin and has been used for well over a hundred years as a robust form of food packaging and beverage cans [10]. Dissolution of metallic tin, especially from the inside of a can body into the food content, has a major influence on the food quality and may cause toxicological effects [11]. The provisional tolerable weekly intake for tin is 14 mg/kg of body weight and the recommended maximum permissible levels of tin in food are typically 250 mg/kg (200 mg/kg in the UK) for solid foods and 150 mg/kg for beverages [10].

The corrosion of tin in contact with acidic environments is attributed to the reversal of its polarity and it becoming anodic to iron, since tin is widely used as a protective coating material for iron in acidic media, thereby dissolving the latter [13, 14]. The factors that mainly affect the internal corrosion of food cans include the properties of tinplate, the nature of the food process and the processing and conditions [14]. To avoid corrosion attack, different chemical compounds are added to the aggressive solutions. The most utilized inhibitors in the food industry are nitrites and nitrates [15]. Fortunately, the dissolution of tin in most cases is accompanied by an oxidation step to form a passive film that can protect the metal surface from further corrosion. The thickness of the passive film and its stability is dependent mainly on its formation conditions [14, 16, 17]. Passivation of tin in the

presence of carboxylic acids present in different foodstuffs has also been investigated [11].

This study investigates the inhibition efficiency of carboxylic acids (palmitic and stearic) on the corrosion of tin in a 0.5 M NaCl solution as a corrosive medium. The surface modification of tin by the formation of carboxylic acid self-assembled monolayers (SAMs) is performed using simple immersion and dip-coating methods with an ethanolic solution of carboxylic acid. Potentiodynamic polarization and electrochemical impedance spectroscopy (EIS) are both applied for the investigation. Fourier transform infrared (FTIR) spectroscopy, optical imaging and quantum chemical calculations are applied to provide insight into the inhibition behavior.

## 2. EXPERIMENTAL

The tin rod, 99.99 % obtained from Goodfellow, UK, sealed into a glass tube with Polirepar S with a surface area of 0.235 cm<sup>2</sup> was used as the working electrode. Before each measurement, the working electrode was abraded with SiC paper (#800 to #2000 grit), followed by ultrasonic cleaning with ethanol and redistilled water and drying in a stream of nitrogen.

The supporting electrolyte was a 0.5 mol dm<sup>-3</sup> NaCl solution of pH 6.0 (adjusted with 0.1 mol dm<sup>-3</sup> HCl). The solution was prepared using pro analysis purity grade chemicals (Kemika, Croatia) and redistilled water. The carboxylic acids used in the study were 1 mmol dm<sup>-3</sup> alcoholic solutions of palmitic acid (CH<sub>3</sub>(CH<sub>2</sub>)<sub>14</sub>COOH, PA) and stearic acid (CH<sub>3</sub>(CH<sub>2</sub>)<sub>16</sub>COOH, SA) (Sigma-Aldrich, ≥ 98.5 %).

The surface modification of tin by the carboxylic acid coating, i.e. the formation of carboxylic acid SAMs at the tin surface, was performed by simple immersion and dip-coating methods. For the simple immersion method, the freshly prepared electrode was immersed in the ethanolic solution of the corresponding acid at 21 ± 2 °C for 24 h, rinsed with distilled water and air dried. For the dip-coating method onto a freshly prepared tin surface, the coating was formed by dipping the samples into the ethanolic solution of the corresponding acid at 21 ± 2 °C, which remained immersed for 15 min, pulling them out at a speed of ~1 cm min<sup>-1</sup> and drying at 85 °C for 4 h in a regular air-convection oven. The multilayered coatings on tin were prepared by cycling the above procedure. A schematic of the dip-coating method is shown in Figure 1. Dip coating is a technique that consists of four stages: dipping, immersion, withdrawing and drying. This technique offers numerous ad-

vantages, including inexpensive setup, process simplicity, uniform deposition, low processing temperature and the ability to coat complex shapes and patterns. Heat treatment of the coated substrate is required to densify the coating layer and to eliminate porosity [18].

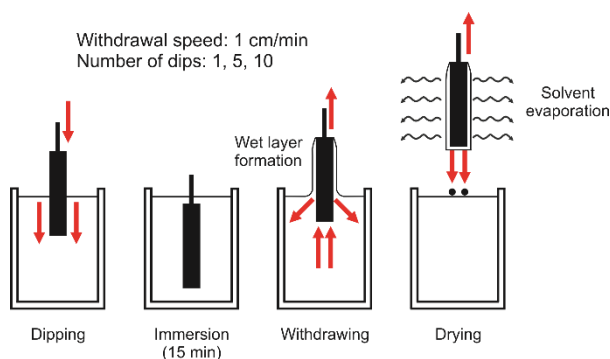


Fig. 1. Schematic illustration of dip-coating process

The corrosion behavior of tin was examined by EIS and potentiodynamic polarization measurements. All electrochemical experiments were performed in a standard three-electrode cell (PAR, Corrosion Cell System) at  $21 \pm 2$  °C in a  $0.5 \text{ mol dm}^{-3}$  NaCl solution of pH 6.0. These measurements were carried out using a Solartron SI 1287 electrochemical interface and a Solartron SI 1255 frequency response analyzer controlled by a personal computer. The counter electrode was a large area platinum electrode and the reference electrode, to which all potentials in the study are referred, was Ag|AgCl, with  $3.0 \text{ mol dm}^{-3}$  KCl ( $E = 0.210 \text{ V}$  vs. standard hydrogen electrode). Both the potentiodynamic ( $1 \text{ mV s}^{-1}$ ) and EIS measurements were performed after an immersion period of 1 h. Potential-time measurements show that the steady-state potential values were established inside this time interval.

EIS measurements were performed at the open circuit potential ( $E_{\text{OCP}}$ ) of the working electrodes (uncoated and coated) in the NaCl solution, with an *ac* voltage amplitude of  $\pm 5 \text{ mV}$  in a frequency range from 100 kHz to 30 mHz. Impedance data were fitted by a suitable electrical equivalent circuit (EEC) model, employing the complex non-linear least squares fit analysis [19] offered by Solartron ZView® software. The fitting quality was evaluated by the chi-squared and relative error values, which were of the order of  $10^{-3}$ – $10^{-4}$  and below 5 %, respectively, indicating that the agreement between the proposed EEC model and the experimental data was good.

The polarization curves,  $E$  against  $j$ , were obtained using the linear potential sweep technique

at a scan rate of  $v = 1 \text{ mV s}^{-1}$  after a 1 h immersion in the  $0.5 \text{ mol dm}^{-3}$  NaCl solution at  $21 \pm 2$  °C in a wide potential range ( $E_{\text{OCP}}/-250 \text{ mV}/E_{\text{OCP}}/+250 \text{ mV}$ ) starting from the  $E_{\text{OCP}}$  to the cathodic direction, then back to  $E_{\text{OCP}}$ , and in the anodic direction.

The FTIR measurements were performed using horizontal attenuated total reflectance method on a PerkinElmer Spectrum One FTIR spectrometer. The spectra were recorded in the range of 4000 to  $650 \text{ cm}^{-1}$  with a scan resolution of  $4 \text{ cm}^{-1}$ .

The surfaces of the working electrode, unmodified and modified, were photographed using a Canon EOS 550 d digital camera in order to visualize the carboxylate coating on the Sn surface. A metallurgical microscope (A 13.0908-A) with a 200× magnification was also used for more in-depth visualization of the modified surface morphology.

Molecular modeling of the carboxylic acid molecules was performed using the semiempirical program from HyperChem 6.0.3.

In order to understand the mechanism of corrosion inhibition, the adsorption behavior of carboxylic acids on the metal surface must be known. For SA, the adsorption isotherm that fits the experimental results was investigated, i.e. the surface coverage data was fitted to different adsorption isotherms. The surface coverage was calculated from the measured values of the corrosion current densities obtained by the Stern-Geary method measured in carboxylic acid free and carboxylic acid containing  $0.5 \text{ mol dm}^{-3}$  NaCl solutions of pH 6.0. Different concentrations of carboxylic acids in the range of  $1$ – $5 \times 10^{-3} \text{ mol dm}^{-3}$  were used. SA was applied on the electrode surface within 30 min of immersion at  $21 \pm 2$  °C under stirring with a magnetic stirrer.

The surface coverage,  $\theta$ , is calculated using  $\theta = [(j - j_{\text{inh}}) / j] \times 100$ , where  $j$  and  $j_{\text{inh}}$  are the corrosion current densities before and after the corrosion inhibition process, respectively.

### 3. RESULTS AND DISCUSSION

#### 3.1. EIS measurements

The EIS measurements were performed to obtain relevant data regarding the barrier properties of the coating-modified tin electrode surface in the NaCl solution. The EIS spectra of the uncoated and coated tin electrodes recorded in the  $0.5 \text{ mol/dm}^3$  NaCl solution at the open circuit potential and room temperature are shown in Figures 2 and 4.

In the Nyquist plots (Figs. 2 and 4), a capacitive semicircle with a diameter equal to the polarization resistance is observed. The value of

polarization resistance is an indicator of corrosion resistance, which is inversely proportional to the corrosion rate. Equivalent circuit modelling was performed based on the EIS results. The numerical values of the impedance parameters are listed in Tables 1 and 2.

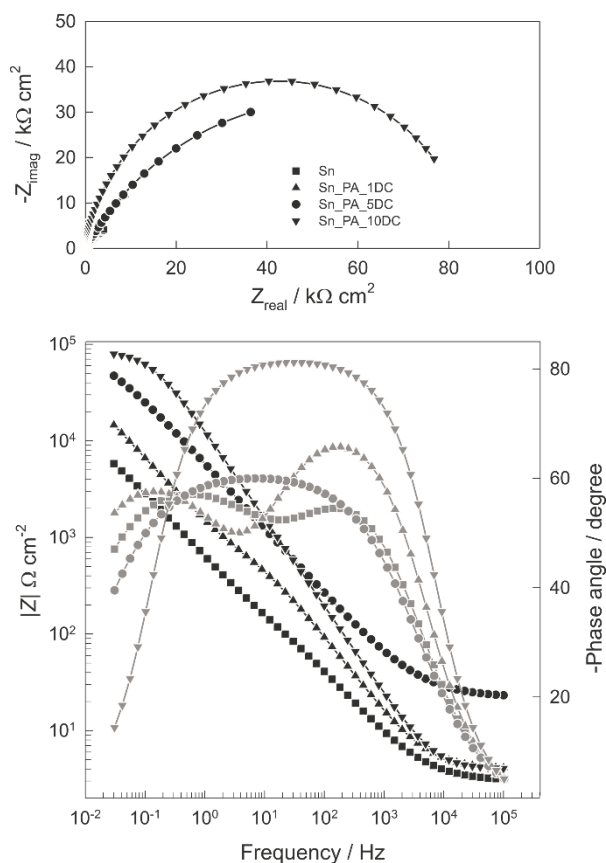


**Fig. 2.** Impedance spectra of uncoated and coated tin electrodes recorded at  $E_{OCP}$  and room temperature in  $0.5 \text{ mol/dm}^3$  NaCl solution at pH 6. The PA film was formed by the dip-coating method (one, five and ten cycles of immersion/drying at  $85^\circ\text{C}$ ).

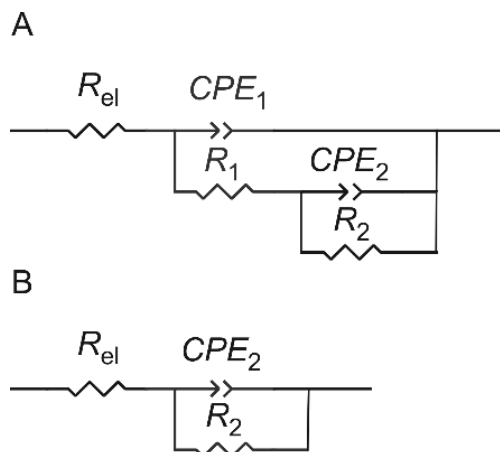


**Fig. 3.** Equivalent electric circuits used to fit impedance data

In the EEC (Fig. 3) with two time constants, which are clearly resolved in the phase angle versus  $\log f$  dependence in Figure 2 (EEC denoted A), the first time constant ( $Q_1R_1$ ), in the high and medium frequency ranges, is related to the properties of the outer part of the porous spontaneously formed oxide film.  $R_1$  is the charge transfer resistance within the pore at the oxide|electrolyte interface and  $Q_1$  is a constant phase element representing the interfacial capacity of the film pore walls. The second time constant ( $Q_2R_2$ ) in the low frequency range describes the impedance of the barrier oxide layer + SAM.  $R_{el}$  corresponds to the electrolyte resistance ( $R_{el} = 4 \Omega \text{ cm}^2$ ).

In the EEC (Fig. 3) with one time constant (EEC denoted B), the  $R_2$ - $Q_2$  parallel combination is connected in series with the electrolyte resistance,  $R_{el}$ .  $R_2$  is the oxide + SAM resistance and  $Q_2$  is a constant phase element that represents the capacity of the carboxylate SAM. The capacitance is in EECs expressed in terms of the constant phase element (CPE) [20] due to the frequency dispersion (mostly attributed to the "capacitance dispersion"). Its impedance is equal to  $Z(\text{CPE}) = [(Q(j\omega)^n)^{-1}]$ , where  $Q$  is a constant,  $\omega$  is the angular frequency and  $n$  is the CPE power. When  $n = 1$ ,  $Q$  represents the pure capacitance, while for  $n \neq 1$ , the system shows behavior that has been attributed to the surface heterogeneity [21] or to the continuously distributed time constants for charge transfer reactions [22].

Figure 2 shows the results of the EIS measurements obtained for the uncoated and PA film coated tin electrodes formed by the dip-coating method. From the Nyquist plot, it is evident that the diameter of the capacitive semicircle grows with the number of application cycles of the dip-coating/drying procedure. The highest polarization resistance, i.e., the highest corrosion resistance, is indicated for the Sn electrode coated with a PA film formed after ten cycles of the dip-coating/drying procedure. From the data presented in Table 1, it is evident that with increasing dip-coating/drying cycles, the polarization resistance ( $R_p = R_1 + R_2$ ) of the protective PA film increases. In addition, the numerical values of the CPE are less than those registered for uncoated tin and decrease with increasing cycles. This change may be influenced by increasing film thickness. The CPE numerical values of  $0.70 < n < 1$  indicate inhomogeneity at a microscopic level at the metal|electrolyte interface (surface roughness, adsorbed species and so on). This study also confirmed the dip-coating method itself, as one of the methods for formation of a protective carboxylic

acid film on the tin surface that can significantly increase the barrier properties of the passive film, in order to protect tin from the corrosive chloride ions. The protection efficiency percentage (PE%) of the carboxylic acid films was calculated from  $PE \% = [(R_{p,CA} - R_p) / R_{p,CA}] \times 100$ , where  $R_p$  and  $R_{p,CA}$  represent the polarization resistances of spontaneously passivated tin and polarization resistanc-

es of tin coated with carboxylic acid film, respectively. A PE equal to 76 % for the electrode coated with a PA film formed after ten cycles of the dip-coating/drying procedure, while for a lower number of cycles, the PE decreases. Thus, for example, for the electrode coated with a PA film formed after five cycles of the dip-coating/drying procedure is ~74 %.

Table 1

*Impedance parameters and protection efficiency percentage (PE%) for uncoated and coated tin electrodes obtained in 0.5 mol/dm<sup>3</sup> NaCl solution at E<sub>OCP</sub>. The PA film was formed by the dip-coating method (one, five and ten cycles).*

|                   | $10^5 \times Q_1 / \Omega^{-1} \text{cm}^{-2} \text{s}^n$ | $n_1$ | $R_1 / \Omega \text{cm}^2$ | $10^5 \times Q_2 / \Omega^{-1} \text{cm}^{-2} \text{s}^n$ | $n_2$ | $R_2 / \text{k}\Omega \text{cm}^2$ | PE / % |
|-------------------|---|-------|----------------------------|---|-------|------------------------------------|--------|
| <b>Sn</b>         | 22.4  | 0.72  | 233                        | 23.8  | 0.66  | 20.2                               | –      |
| <b>Sn_PA_1DC</b>  | 5.8   | 0.81  | 896                        | 15.6  | 0.69  | 75.6                               | 73     |
| <b>Sn_PA_5DC</b>  | –   | –     | –                          | 4.8   | 0.68  | 80.1                               | 74     |
| <b>Sn_PA_10DC</b> | –   | –     | –                          | 1.5   | 0.91  | 84.9                               | 76     |

$R_{el} = 4 \Omega \text{ cm}^2$

PA: palmitic acid; 1 (5 or 10) DC: 1 (5 or 10) cycle(s) of immersion / drying at 85°

Table 2

*Impedance parameters and protection efficiency percentage (PE%) for uncoated and coated tin electrodes obtained in 0.5 mol/dm<sup>3</sup> NaCl solution at E<sub>OCP</sub>. The PA and SA films were formed by the dip-coating (ten cycles) and immersion methods (24 h).*

|                   | $10^5 \times Q_1 / \Omega^{-1} \text{cm}^{-2} \text{s}^n$ | $n_1$ | $R_1 / \Omega \text{cm}^2$ | $10^5 \times Q_2 / \Omega^{-1} \text{cm}^{-2} \text{s}^n$ | $n_2$ | $R_2 / \text{k}\Omega \text{cm}^2$ | PE / % |
|-------------------|---|-------|----------------------------|---|-------|------------------------------------|--------|
| <b>Sn</b>         | 22.4  | 0.72  | 233                        | 23.8  | 0.66  | 20.2                               | –      |
| <b>Sn_PA_10DC</b> | –   | –     | –                          | 1.5   | 0.91  | 84.9                               | 76     |
| <b>Sn_PA</b>      | 2.4   | 0.91  | 3226                       | 4.4   | 0.59  | 60.8                               | 68     |
| <b>Sn_SA_10DC</b> | –   | –     | –                          | 3.5   | 0.88  | 159.1                              | 87     |
| <b>Sn_SA</b>      | 1.3   | 0.91  | 4359                       | 1.2   | 0.62  | 128.8                              | 85     |

$R_{el} = 4 \Omega \text{ cm}^2$

PA: palmitic acid; SA: stearic acid; 10DC: 10 cycles of immersion / drying at 85°

Figure 4 shows the impedance spectra of the uncoated and coated Sn electrodes. The Sn electrode was coated by the carboxylic acid film (PA or SA) formed by the two methods. All spectra are almost the same shape as those shown in Figure 2 and are therefore fitted to the same EECs. From the data given in Table 2 and Figure 4, it can be seen that the electrode coated with a PA or SA film formed by one method or another has a higher capacitive semicircle, i.e. polarization resistance, compared to the polarization resistance of the un-

coated Sn electrode. Its significant increase points to a change in the film composition, i.e., adsorption of carboxylic acid, which is responsible for increasing the barrier properties. From the above data, it is also evident that as the length of the hydrocarbon chain increases, the capacitive semicircle, i.e. the polarization resistance of the tin electrode, increases [6]. Thus, the largest numerical value of PE equal to 87 % was obtained for the Sn electrode coated with a SA film formed after ten cycles of the dip-coating/drying procedure.

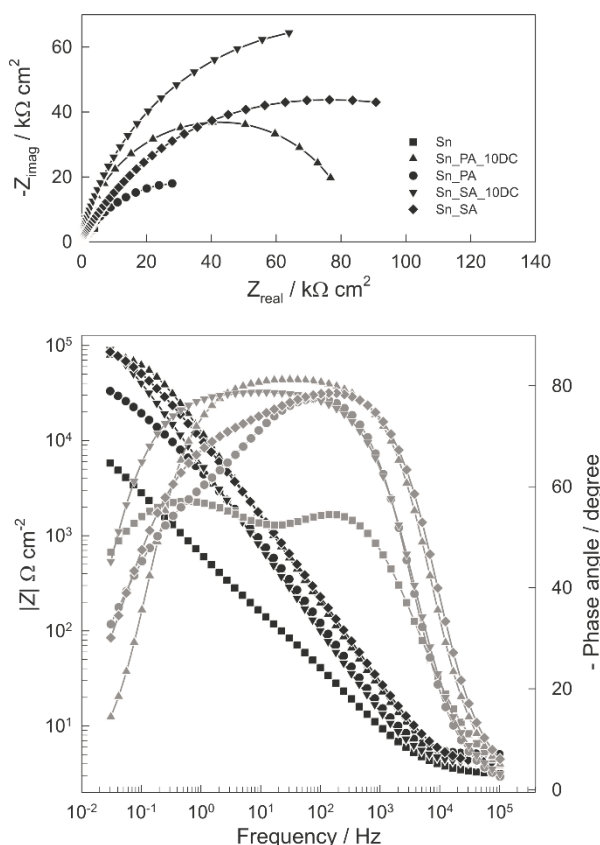


**Fig. 4.** Impedance spectra of uncoated and coated tin electrodes recorded at  $E_{OCP}$  and at room temperature in 0.5 mol/dm<sup>3</sup> NaCl solution. PA and SA films were formed by the dip-coating (ten cycles of immersion/drying at 85 °C) and immersion methods (24 h).

### 3.2. Potentiodynamic polarization measurements

Polarization measurements were carried out to gain knowledge regarding the kinetics of the cathodic and anodic reactions and to determine how the inhibitory effect acted. Figure 5 shows the polarization curves of the uncoated and coated tin electrodes in the 0.5 mol/dm<sup>3</sup> NaCl solution. The Sn electrode was coated with carboxylic acid (PA/SA) films formed by dip coating or by simple immersion. Measurements were carried out over a wide range of potentials around the  $E_{OCP}$  at a scan rate of 1 mV/s and room temperature. By increasing the number of dip-coating/drying cycles, the values of the anodic and cathodic corrosion current density of the tin electrode also decreased, resulting in an increase in corrosion resistance (not shown here).

From Figure 5 it can be seen that the values of the cathodic and anodic current density of the tin electrode coated with carboxylic acid (PA/SA) films formed by both deposition methods are visibly decreased. In the anode branch, the current densities of the coated tin electrode are character-

ized by a passive area, followed by a sharp increase in current density (film breakdown potential), indicating that the surface film suppresses the reaction of the anodic oxidation. In the cathode branch, values of Tafel slopes ranging from  $-157$  to  $-229$  mV decade<sup>-1</sup> indicate that the hydrogen reduction reaction takes place at electrodes covered by the surface film [5, 23].

Table 3 summarizes the electrochemical kinetic parameters of the Tafel extrapolations ( $E_{corr.}$ ,  $b_c$ ,  $b_a$ ,  $j_{corr.}$  and PE %). The PE % of the carboxylic acid films was calculated by  $PE / \% = [(j_{cor.} - j_{cor.,CA}) / j_{cor.}] \times 100$ , where  $j_{cor.}$  and  $j_{cor.,CA}$  represent the corrosion current density of spontaneously passivated tin and corrosion current density of tin coated with carboxylic acid films, respectively. The increase in dip-coating/drying cycles results in a considerable regular decrease in corrosion current density ( $j_{cor.}$ ) and a regular increase in PE %, where a PE % of 96 % was achieved for the SA film formed by the dip-coating method (ten cycles). The extrapolated corrosion current density is affected by the length of hydrocarbon chains of the carboxylic acid (Table 3). The polarization curves shown in Figure 5 and the values of corrosion parameters shown in Table 3 once again **have** confirmed the protective effect of carboxylic acids on the corrosion of tin in the 0.5 mol/dm<sup>3</sup> NaCl electrolyte solution.

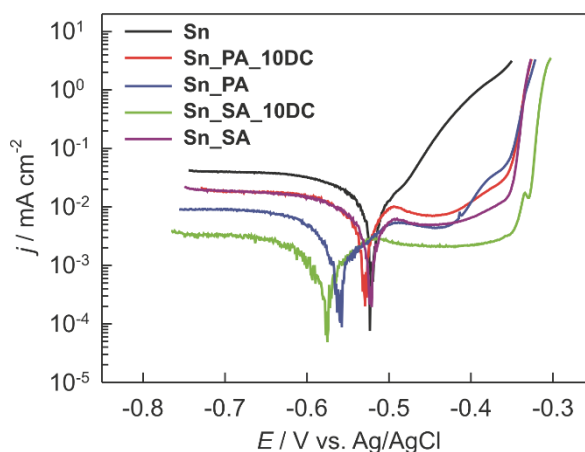


**Fig. 5.** Tafel plots for uncoated and coated tin electrodes recorded in 0.5 mol/dm<sup>3</sup> NaCl solution for pH 6 and  $v = 1$  mV s<sup>-1</sup>. PA and SA films were formed by the dip-coating (ten cycles of immersion/drying at 85 °C) and immersion methods (24 h).

It is also observed that the addition of the tested inhibitors retards both the cathodic and anodic reactions; however, the cathodic reactions are comparatively more affected than the anodic ones, suggesting that the investigated inhibitors are mixed type inhibitors and predominantly act as cathodic inhibitors [24, 25]. Other films have also

shown high efficiencies, so both deposition methods have shown to be effective for forming films that successfully prevent the corrosion of the tested tin electrode in this electrolyte. The corrosion rate decrease is attributed to inhibitor adsorption on active metal sites [24], present on the tin surface, which is the primary step in achieving inhibition in

the NaCl solution. The coating film provides corrosion protection to metallic substrates by acting as a barrier against electron and ion diffusion [18], thus reducing electrochemical reactions at the interface of Sn and electrolyte. The obtained results from Tafel polarization showed good agreement with the EIS measurements.

Table 3

Corrosion kinetic parameters for uncoated and coated tin electrodes recorded in  $0.5 \text{ mol/dm}^3$  NaCl solution at pH 6 and  $v = 1 \text{ mV s}^{-1}$ . The PA and SA films were formed by the dip-coating (ten cycles) and immersion methods (24 h).

|            | $-b_c /$<br>mV | $b_a /$<br>mV | $j_{\text{corr.}} /$<br>$\mu\text{A cm}^{-2}$ | $-E_{\text{corr.}} /$<br>mV | PE / % |
|------------|----------------|---------------|---|-----------------------------|--------|
| Sn         | 157            | 93            | 12.7  | 524                         | –      |
| Sn_PA_10DC | 214            | 41            | 2.9   | 532                         | 77     |
| Sn_PA      | 225            | 13            | 1.0   | 567                         | 92     |
| Sn_SA_10DC | 229            | 11            | 0.5   | 575                         | 96     |
| Sn_SA      | 216            | 28            | 2.3   | 525                         | 82     |

PA: palmitic acid; SA: stearic acid; 10DC: 10 cycles of immersion / drying at  $85^\circ\text{C}$

### 3.3. Electrode surface analysis

#### 3.3.1. FTIR measurements

After the electrochemical measurements, FTIR analysis of the tin electrode surface was performed to determine the presence and some structural characteristics of the protective SA surface film. Figure 6 shows the FTIR spectra of the tin plate on which SA was applied with ten dip-coating/drying cycles) and the tin plate on which SA was applied by the immersion method (24 h immersion in SA solution).

In the FTIR spectra, the peaks at  $2852 \text{ cm}^{-1}$  and  $2922 \text{ cm}^{-1}$  assigned to symmetric ( $2852 \text{ cm}^{-1}$ ) and asymmetric ( $2922 \text{ cm}^{-1}$ ) C–H stretching vibrations, respectively, indicate that SA has been successfully adsorbed [26]. Peaks at  $\sim 1540 \text{ cm}^{-1}$  are attributed to the stretching vibration of carboxyl groups ( $-\text{COO}^-$ ) [6, 27, 28]. In the FTIR spectra of a tin plate on which SA was applied by the dip-coating method, the C–O stretching band occurs at  $1464 \text{ cm}^{-1}$  while the band at  $1413 \text{ cm}^{-1}$  is related to stretching vibrations of the C–O–H bond [29]. In the FTIR spectra of a tin plate on which SA was applied by the immersion method, the peak at  $1709 \text{ cm}^{-1}$  is carbonyl group C=O stretching vibration absorption peak [27, 29]. Compounds containing a carboxyl group act as highly effective inhibitors for chloride ion penetration through a passive surface film exist on the various metals and alloys, due to their competitive adsorption on the oxide

film, since carboxylate ions are harder bases than chloride ions [6, 30].

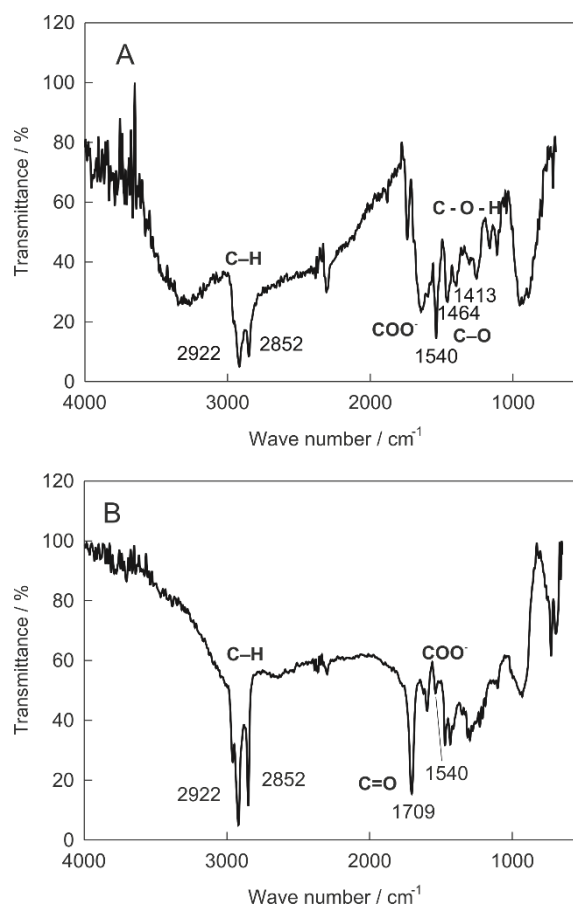
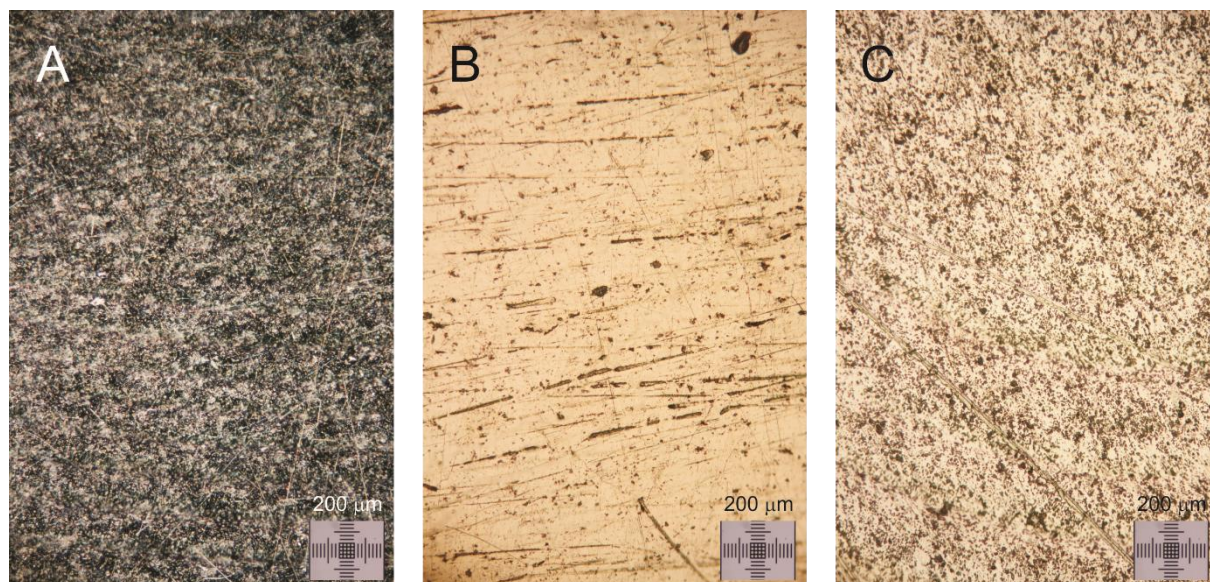


Fig. 6. FTIR spectra of tin coated with SA film formed by (A) dip-coating and (B) immersion methods

### 3.3.2. Optical microscopy analysis

Optical microscopy analysis of the tin electrode surface was performed after the potentiodynamic polarization measurements. The optical image of uncoated and coated tin sample surfaces is shown in Figure 7. The SA SAM was formed by the dip-coating (ten cycles) and immersion meth-

ods (24 h). From the microscopic images, it can be seen that both methods lead to the formation of a SA film homogeneously distributed on the tin electrode surface. The SA film almost completely covers electrode surface that is then barely visible below the film, which is an indicator of good SA film adhesion.



**Fig. 7.** Optical image of uncoated tin sample surface (A), tin sample surface coated with SA SAM formed by dip-coating (ten cycles) (B) and immersion methods (24 h) (C)

### 3.4. Adsorption isotherm

The effectiveness of different carboxylic acids as corrosion inhibitors is also related to the extent of adsorption of their molecules and how these molecules can cover the metal surface and protect it from continuous corrosion. The adsorption process depends on the structure of the inhibitor molecules, the surface charge of the metal and the constituents of the electrolyte [11]. The numerical values of  $\theta$  for different concentrations of SA were used in determining the isotherm, which described the best adsorption of stearate ions on the tin surface. Figure 8 shows that the experimental data fit best (regression coefficient of 0.999) the Langmuir adsorption isotherm:  $c/\theta = 1/K_{\text{ads}} + c$ , where  $K_{\text{ads}}$  is the adsorption constant in  $\text{dm}^3 \text{mol}^{-1}$  and  $c$  is the SA concentration in  $\text{mol dm}^{-3}$ . The relationship between the adsorption constant ( $K_{\text{ads}}$ ) and the Gibbs free energy of adsorption ( $\Delta G_{\text{ads}}$ ) is given by:

$$K_{\text{ads}} = \frac{1}{55.5} \exp\left(\frac{-\Delta G_{\text{ads}}}{RT}\right), \quad (1)$$

where  $R$  is the universal gas constant,  $T$  is the absolute temperature,  $T = 298 \text{ K}$ , and 55.5 is the concentration of water in the solution in  $\text{mol dm}^{-3}$ .

The Langmuir adsorption isotherm has been reported for the adsorption of SA on metal surfaces [24]. The adsorption constant and Gibbs free energy were determined to be  $K_{\text{ads}} = 2578 \text{ dm}^3 \text{mol}^{-1}$  and  $\Delta G_{\text{ads}} = -29.4 \text{ kJ mol}^{-1}$ . The negative value of  $\Delta G_{\text{ads}}$  suggests that the SA adsorbs spontaneously on the tin surface and indicates an electrostatic interaction between the metal surfaces and carboxylic acid. Generally, the values of  $\Delta G_{\text{ads}}$  up to  $-20 \text{ kJ mol}^{-1}$  are consistent with electrostatic interactions between molecular ions and the substrates, while those around  $-40 \text{ kJ mol}^{-1}$  involve chemisorption [31, 32].

The quantum chemical approach was used to obtain a better understanding of the relationship between the investigated molecules inhibition efficiency and molecular structure. The insert of Figure 8 shows an optimized structure of the SA molecules with a density of electrons in the highest occupied molecular orbital (HOMO). According to the description of the frontier orbital theory, the



HOMO is often associated with the electron donating ability of an inhibitor molecule. High  $E_{\text{HOMO}}$  values indicate that the molecule tends to donate electrons to the metal with unoccupied molecule orbitals [1]. This result indicates that the adsorption of inhibitor onto the metal surface can occur on the basis of donor-acceptor interactions between inhibitors'  $\pi$  electrons and the vacant d-orbitals of the metal surface atoms. Investigated carboxylic acids have the highest density of electrons in the carboxylic group and it can be considered as a reaction center for binding to the surface oxide [6, 24].

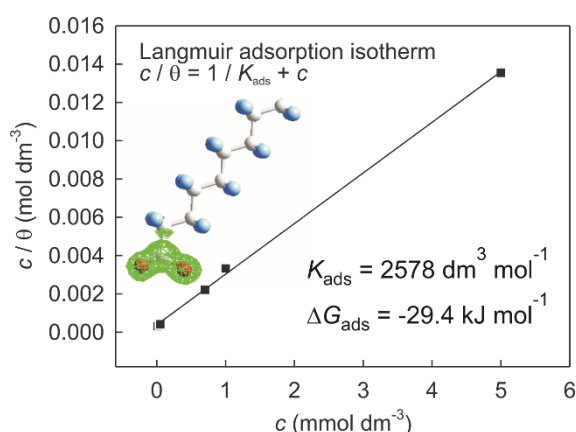


**Fig. 8.** Langmuir adsorption isotherm for tin electrode in a 0.5 mol/dm<sup>3</sup> NaCl solution containing SA. The insert shows the optimized structures of the SA molecules with the density of electrons in the highest occupied molecular orbital.

#### 4. CONCLUSIONS

Tin electrode surfaces were modified with organic acid SAMs formed by dip-coating (one, five and ten cycles) and immersion methods. EIS and potentiodynamic polarization results show that the carboxylic acid film formed either by the dip-coating or immersion methods significantly increases the corrosion resistance of the tin electrode in a 0.5 M NaCl solution. The potentiodynamic polarization curves indicate that these carboxylic acids act as mixed-type inhibitors, with more polarized cathodic than anodic curves. The adsorption of stearic acid follows the Langmuir adsorption isotherm and the free energy of adsorption was calculated to be  $-29.4 \text{ kJ mol}^{-1}$ , which reveals physical adsorption. FTIR spectroscopy and optical imaging confirmed the stability and adhesion of the carboxylic acid protective SAMs. The highest corrosion protection efficiency was obtained for the tin electrode modified with the SA film formed by the dip-coating method (ten cycles).

**Acknowledgements.** The authors gratefully acknowledge Full Prof. Dr. Zoran Grubač from the Department of General and Inorganic Chemistry, Faculty of Chemistry and Technology, University of Split, Croatia, for his contribution to implementation of the dip-coating method.

**Funding.** The author(s) received no financial support for the research, authorship and/or publication of this article.

#### REFERENCES

- [1] B. E. Amitha Rani, B. B. J. Basu, Review article: Green inhibitors for corrosion protection of metals and alloys: an overview, *Int. J. Corros.*, 1–15 (2012). DOI: <https://doi.org/10.1155/2012/380217>
- [2] A. Sahaya Raja, S. Rajendran, J. Sathiyabama, P. Angel, Corrosion control by aminoacetic acid (glycine): an overview, *Int. J. Innov. Res. Sci. Eng. Technol.* **3**, 11455–11467 (2014). <http://www.rroij.com/open-access/corrosion-control-by-aminoacetic-acid-glycine-an-overview.pdf>
- [3] L. Vrsalović, S. Gudić, D. Gracić, I. Smoljko, I. Ivanić, M. Kliškić, E. E. Oguzie, Corrosion protection of copper in sodium chloride solution using propolis, *Int. J. Electrochem. Sci.* **13**, 2102–2117 (2018). DOI: <https://doi.org/10.20964/2018.02.71>
- [4] M. Metikoš-Huković, R. Babić, I. Škugor Rončević, Z. Grubač, Surface modifications of the Mg alloy by self-assembled monolayers of fatty acids, *ECS Trans.* **41**, 81–91 (2012). DOI: [10.1149/1.3692438](https://doi.org/10.1149/1.3692438)
- [5] Z. Grubač, I. Škugor Rončević, M. Metikoš-Huković, R. Babić, M. Petravić, R. Peter, Surface modification of biodegradable magnesium alloys, *J. Electrochem. Soc.* **159**, C253–C258 (2012), DOI: [10.1149/2.047206jes](https://doi.org/10.1149/2.047206jes)
- [6] I. Škugor Rončević, N. Vladislavić, M. Buzuk, Surface Modifications of the biodegradable magnesium based implants with self-assembled monolayers formed by T-BAG method, *Acta Chim. Slov.* **65**, 1–11 (2018). DOI: <https://doi.org/10.17344/acsi.2018.4400>
- [7] S. A. Umoren, U. M. Eduok, Application of carbohydrate polymers as corrosion inhibitors for metal substrates in different media: a review, *Carbohydr. Polym.* **140**, 314–341 (2016). DOI: <https://doi.org/10.1016/j.carbpol.2015.12.038>
- [8] I. Obot, N. Obi-Egbedi, S. Umoren, Antifungal drugs as corrosion inhibitors for aluminium in 0.1 M HCl, *Corros. Sci.* **51**, 1868–1875 (2009). DOI: <https://doi.org/10.1016/j.corsci.2009.05.017>
- [9] H. Elgahawi, M. Gobara, A. Baraka, W. Elthalabawy, Eco-friendly corrosion inhibition of aa2024 in 3.5% nacl using the extract of *Linum usitatissimum* seeds, *J. Bio. Tribo. Corros.* **3:55**, 1–13 (2017). DOI: <https://doi.org/10.1007/s40735-017-0116-x>
- [10] S. Blunden, T. Wallace, Tin in canned food: a review and understanding of occurrence and effect, *Food Chem. Toxicol.* **41**, 1651–1662 (2003). DOI: [10.1016/s0278-6915\(03\)00217-5](https://doi.org/10.1016/s0278-6915(03)00217-5)
- [11] R. M. El-Sherif, W. A. Badawy, Mechanism of corrosion and corrosion inhibition of tin in aqueous solutions containing tartaric acid, *Int. J. Electrochem. Sci.* **6**, 6469–6482 (2011). DOI: <http://electrochemsci.org/papers/vol6/6126469.pdf>

- [12] B. F. Gannetti, P. T. Sumodjo, T. Rabockai, A. Souza, J. Barboza, Electrochemical dissolution and passivation of tin in citric acid solution using electron microscopy techniques, *Electrochim. Acta* **37**, 143–148 (1992). DOI: [https://doi.org/10.1016/0013-4686\(92\)80023-F](https://doi.org/10.1016/0013-4686(92)80023-F)
- [13] A. Albu-Yaron, A. Feigin, Effect of growing conditions on the corrosivity and ascorbic acid retention in canned tomato juice, *J. Sci. Food Agric.* **59**, 101–108 (1992). DOI: <https://doi.org/10.1002/jsfa.2740590115>
- [14] M. A. Quraishi, F. A. Ansari, D. Jamal, Corrosion inhibition of tin by some amino acids in citric acid solution, *Indian J. Chem. Techn.* **11**, 271–274 (2004). <http://hdl.handle.net/123456789/16779>
- [15] K. Galić, M. Pavić, N. Ciković, The effect of inhibitors tin in sodium on the corrosion chloride of solution, *Corros. Sci.* **36**, 785–795 (1994). DOI: [https://doi.org/10.1016/0010-938X\(94\)90170-8](https://doi.org/10.1016/0010-938X(94)90170-8)
- [16] C. M. V. B. Almeida, T. Rabockai, B. F. Giannetti, Inhibiting effect of citric acid on the pitting corrosion of tin, *J. Appl. Electrochem.* **29**, 123–128 (1999). DOI: <https://doi.org/10.1023/A:1003468731553>
- [17] P. E. Avarez, S. B. Ribotta, M. E. Folker, C. A. Gervasi, J. R. Vilche, Potentiodynamic behaviour of tin in different buffer solutions, *Corros. Sci.* **44**, 49–65 (2002). DOI: [https://doi.org/10.1016/S0010-938X\(01\)00032-4](https://doi.org/10.1016/S0010-938X(01)00032-4)
- [18] M. F. Mohd Yusoff, M. R. Abdul Kadir, N. Iqbal, M. A. Hassan, R. Hussain, Dipcoating of poly( $\epsilon$ -caprolactone)/hydroxyapatite composite coating on Ti6Al4V for enhanced corrosion protection, *Surf. & Coat. Technol.* **245**, 102–107 (2014). DOI: <https://doi.org/10.1016/j.surfcoat.2014.02.048>
- [19] B. A. Boukamp, A Nonlinear least squares fit procedure for analysis of immittance data of electrochemical systems, *Solid State Ion.* **20**, 31–44 (1986). DOI: [https://doi.org/10.1016/0167-2738\(86\)90031-7](https://doi.org/10.1016/0167-2738(86)90031-7)
- [20] J. R. Macdonald, *Impedance Spectroscopy: Emphasizing Solid Materials and Systems*, New York, John Wiley & Sons Inc, 1987, pp. 301. DOI: [https://doi.org/10.1016/0584-8539\(88\)80155-7](https://doi.org/10.1016/0584-8539(88)80155-7)
- [21] Z. Lukasc, Evaluation of model and dispersion parameters and their effects on the formation of constant-phase elements in equivalent circuits, *J. Electroanal. Chem.* **464**, 68–75 (1999). DOI: [https://doi.org/10.1016/S0022-0728\(98\)00471-9](https://doi.org/10.1016/S0022-0728(98)00471-9)
- [22] J. R. Macdonald, Power-law exponents and hidden bulk relation in the impedance spectroscopy of solids, *J. Electroanal. Chem.* **378**, 17–29 (1994). DOI: [https://doi.org/10.1016/0022-0728\(94\)87053-5](https://doi.org/10.1016/0022-0728(94)87053-5)
- [23] G. Zorn, I. Gotman, E. Y. Gutmanas, R. Adadi, G. Salitra, C. N. Sukenik, Surface modification of Ti45Nb alloy with an alkylphosphonic acid self-assembled monolayer, *Chem. Mater.* **17**, 4218–4226 (2005). DOI: <https://doi.org/10.1007/s10856-006-0117-7>
- [24] N. Soraya, D. Rayenne, M. Boulanouar, O. Rabah, Structure-corrosion inhibition performance relationship: Application to some natural free acids and antioxidants, *Port. Electrochimica Acta*, **36**, 23–34 (2018). DOI: <https://doi.org/10.4152/pea.201801023>
- [25] A. N. Grassino, J. Halambek, S. Djaković, S. Rimac Brnčić, M. Dent, Z. Grabarić, Utilization of tomato peel waste from canning factory as a potential source for pectin production and application as tin corrosion inhibitor, *Food Hydrocoll.* **52**, 265–274 (2016). DOI: <https://doi.org/10.1016/j.foodhyd.2015.06.020>
- [26] M. D. Porter, T. B. Bright, D. L. Allara, C. E. D. Chidsey, Spontaneously organized molecular assemblies. 4. Structural characterization of n-alkyl thiol monolayers on gold by optical ellipsometry, infrared spectroscopy, and electrochemistry, *J. Am. Chem. Soc.* **109**, 3559–3568 (1987). DOI: <https://doi.org/10.1021/ja00246a011>
- [27] A. Raman, E. Gawalt, Self-assembled monolayers of alkanolic acids on the native oxide surface of SS316L by solution deposition, *Langmuir* **23**, 2284–2288 (2007). DOI: <https://doi.org/10.1021/la063089g>
- [28] M. A. Szymański, M. J. Gillan, The energetics of adsorption of HCOOH on the MgO(100) surface, *Surf. Sci.* **367**, 135–148 (1996). DOI: [https://doi.org/10.1016/S0039-6028\(96\)00870-9](https://doi.org/10.1016/S0039-6028(96)00870-9)
- [29] M. S. Lim, K. Feng, X. Chen, N. Wu, A. Raman, J. Nightingale, E. S. Gawalt, D. Korakakis, L. A. Hornak, A. T. Timperman, Adsorption and desorption of stearic acid self-assembled monolayers on aluminum oxide, *Langmuir* **23**, 2444–2452 (2007). DOI: <https://doi.org/10.1021/la061914n>
- [30] S. Martinez, L. Valek, I. Stipanović Oslaković, Adsorption of organic anions on low-carbon steel in saturated Ca(OH)<sub>2</sub> and the HSAB principle, *J. Electrochem. Soc.* **154**, C671–C677 (2007). DOI: <https://doi.org/10.1149/1.2777882>
- [31] Ž. Petrović, M. Metikoš-Huković, R. Babić, Potential-assisted assembly of 1-dodecanethiol on polycrystalline gold, *J. Electroanal. Chem.* **623**, 54–60 (2008). DOI: <https://doi.org/10.1016/j.jelechem.2008.06.018>
- [32] A. M. Ahmed, Y. A. Aggour, M. A. Shreadah, M. Darweesh, E. Sallam, Anodic corrosion of copper in presence of polymers, *Int. J. Appl. Eng. Res.* **2**, 221–230 (2014). DOI: <https://www.researchgate.net/publication/303372947>